Antonova, A; Eik, M; Puttonen, J

Characterisation of bond between cement paste and steel fibres with different surface roughness using SEM

Published in:
Journal of Microscopy

DOI:
10.1111/jmi.13298

Published: 01/05/2024

Document Version
Publisher's PDF, also known as Version of record

Received: 18 December 2023 | Revised: 21 March 2024 | Accepted: 21 March 2024

DOI: 10.1111/jmi.13298

THEMED ISSUE ARTICLE

Journal of Microscopy RMS

Characterisation of bond between cement paste and steel fibres with different surface roughness using SEM

Anna Antonova[1] | **Marika Eik**[2] | **Jari Puttonen**[1]

[1]Department of Civil Engineering, Aalto University, Espoo, Finland

[2]Estonian Entrepreneurship University of Applied Sciences, Tallinn, Estonia

Correspondence
Anna Antonova, Department of Civil Engineering, Aalto University, Espoo 02150, Finland.
Email: anna.antonova@aalto.fi

Funding information
AaltoENG doctoral programme of the School of Engineering of Aalto University

Abstract

The performance of cementitious composites reinforced with fibres or/and bars depends on the bond strength between inclusion and cementitious matrix. The nature of formation of fibre-matrix bond is crucial for enhancing the reliability and utilisation of reinforced composites. The research provides a review on the recently published result about the changes in the microstructure of cement matrix surrounding steel fibres with different surface roughness, using a scanning electron microscope (SEM) coupled with *k*-means clustering algorithm for image segmentation. The debonding pattern of the fibre-matrix bond after the tensile loading cycles was discussed by observing the amount of adhered cement paste to the pulled out fibre surface with SEM. Therefore, analysis of SEM images enabled to explain the connection between the micro-scale properties of cement paste and fibre after application of cyclic loading.

KEYWORDS

fibre-matrix interface, image processing, interfacial transition zone, load cycles, steel fibres, surface roughness

1 | INTRODUCTION

The structural performance of fibre-reinforced cementitious composites (FRCC) depends on the micro-scale properties of fibres and the surrounding cementitious matrix, known as the interfacial transition zone (ITZ). Similar ITZ is also forming around aggregates and conventional reinforcement bars. The bond between fibres and cement paste defines the stress-transfer mechanisms along their interface, thereby influencing the overall load capacity of the composite.

The fibre size is several times larger than cement grains, which leads to inefficient packing of cement grains, resulting in increased porosity near the fibre surface. The complete dissolution of small grains near fibre surface rapidly saturates the water solution with calcium ions, leaving space for the precipitation of calcium hydroxide (CH).[1–3] The size and the network of pores and the amount of CH, which can easily leach in contact with an aggressive environment, can contribute to the degradation of the fibre-matrix bond, affecting the durability of FRCC. The heterogeneous thickness of ITZ around fibres, caused by bleeding effect or uneven packing of grains, complicates the prediction of the behaviour of the fibre-matrix bond.[4]

The lack of experimental outcomes regarding the relationship between fibre and cement paste properties and their effect on bond formation and load-bearing capacity limit the effective development and implementation of FRC composites in construction. Most of the concrete structures are subjected to live load, which more commonly cause gradual accumulation of damage and material degradation than the occurrence of the ultimate design load. The properties of ITZ may result in discontinuous contact and local stress concentrations under loading.[5] The investigations of fibre-matrix bond under tension were primarily performed under monotonic loading.[6,7] The limited amount of studies in Refs. [8, 9] were testing FRCC and plain concrete under compression load cycles, but further research is required to understand the behaviour of fibre-matrix bond under tensile load cycles.

The current report provides a reflection on the benefits of SEM investigations applied in Refs. [10, 11] and corresponding results. The discussed outcomes and SEM images were used to characterise the microstructure of the ITZ around fibres with different roughness and indicate potential reasons of the degradation behaviour of fibre-matrix bond under non-monotonic loading.

2 | MATERIALS AND METHODS

2.1 | Materials

The surface of the steel fibres with a diameter of 1 mm had initial manufactured roughness, which was achieved with electro-chemical polishing in a solution of ethanol and nitric acid (2:1) at −30°C and sanding with sandpaper with a grit size of 60 μm perpendicularity to fibre length (Figure 5A–C). Then fibres were fixed in a vertical position to minimise the effect of casting direction and bleeding. The cementitious binder with 16% blast furnace slag and 8% limestone was prepared with a water-to-binder ratio of 0.5.

The specimens for microstructural investigations were cast as prisms with a size of $40 \times 40 \times 160$ mm^3, which were demoulded the next day and stored for the following 27 days in relative humidity (RH) of 100%. Then cylinders with the fibre in the centre were drilled out from the prisms, sections of 2–3 mm were cut from the middle of each cylinder and stored in isopropanol for the next 5 days for hydration stoppage. After epoxy impregnation specimens were ground and polished with SiC sandpaper with grades of 1200 and 4000, followed by polishing with diamond suspension with grades of 9, 3 and 1 μm. 6 samples were analysed per fibre with different surface roughness.

In the case of cyclic pull-out test, The samples were cast in mould, which enabled embedding steel fibres to a depth of 30 mm at the centre of cement paste cylinder with a diameter of 45 mm and height of 60 mm. Specimens were demoulded the next day and placed to RH of 100% for the following 27 days. 6 samples were tested per fibre surface with different surface roughness.

A detailed information about the processing of the fibre surfaces and sample preparation are provided in Refs. [10, 11].

2.2 | Methods

The entire interface between cementitious matrix and fibres was captured with a minimum of 16 backscatter electron images (BSE) to analyse the distribution of unhydrated (UH) grains and porosity within the ITZ with an image resolution of 0.117 μm/px (Figure 1A). Porosity and UH grains were segmented from the BSE images as the darkest and the brightest phases, respectively.

Instead of global threshold method, which relies on manually defined thresholds using the histogram of grey-level intensities,[12–14] the k-means clustering algorithm was applied to support accuracy of image segmentation. This algorithm considers pixels as data points, defining the densest regions as local maxima of the point distribution, which are interpreted as the centroids of the clusters. The number of clusters is predefined based on the minimum clustering error (Figure 1B). The update of the cluster centroids stops when the sum of squared distances between the data points and cluster centroid is minimal, as explained in Refs. [15, 16]. This eliminates the challenges associated with threshold detection. The k-means clustering algorithm was applied for the segmentation of cementitious matrix around fibre in Ref. [10] with the steps illustrated in Figure 1. In the case of k-means clustering, the predefined number of five clusters was used based on clustering error calculation, which improved the quality of the segmentation (Figure 1C). The distributions of UH grains and pores were calculated as the area fraction of each phase per 5 μm band width at a distance of 100 μm from the fibre surface (Figure 1D).

Following the determination of the ITZ microstructure around fibres with SEM, the roughness and wetting of the fibre surface were quantified to enhance the reliability of bond analysis. Additionally, SEM was employed to investigate the fibre surface after cyclic pull-out tests, conducted at a loading rate of 1 μm/min. The cyclic loading was applied to simulate a life load, which causes a more common failure of the composite due to accumulated damage before reaching the ultimate design load. Further details of these tests are reported in Ref. [11]. The BSE images were taken from the middle part of each fibre with resolution of 1 μm/px to ensure clear contrast between steel fibre surface and cement paste.

Journal of Microscopy RMS

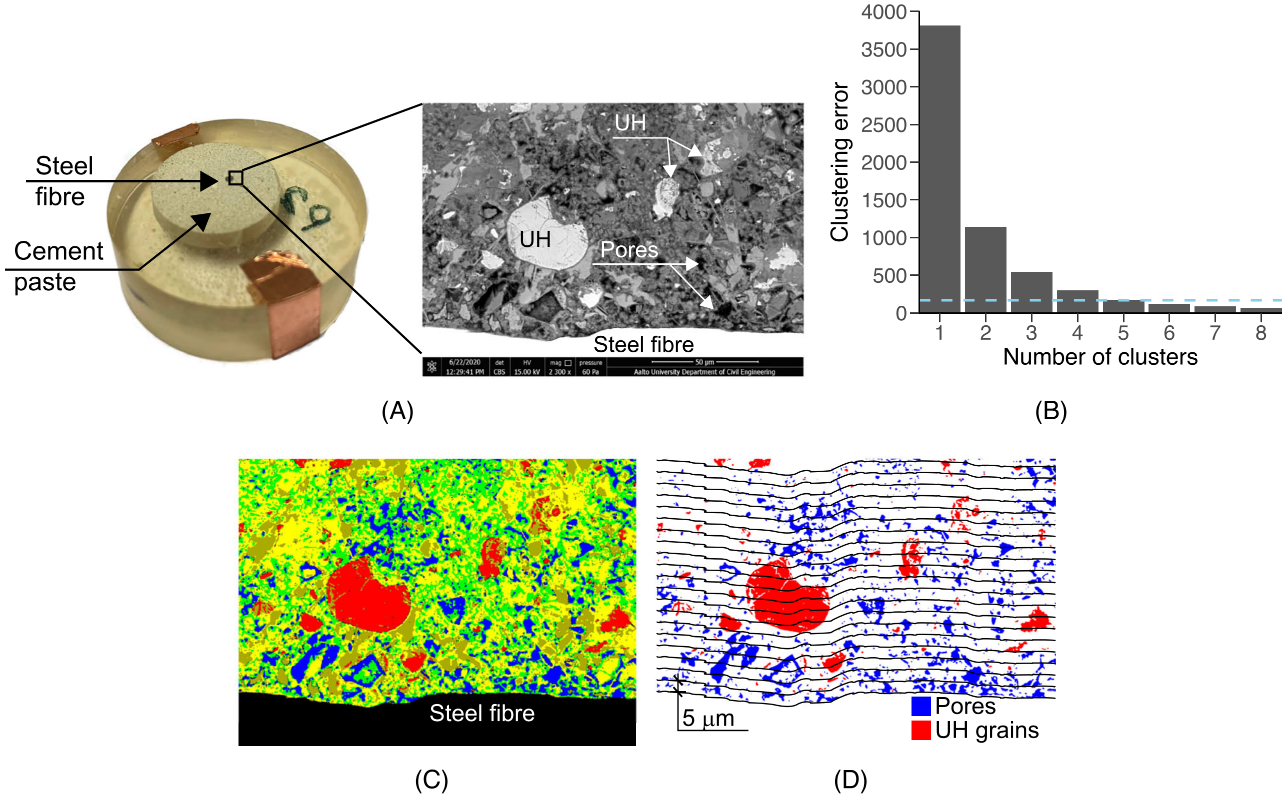

FIGURE 1 (A) An example of specimen studied with SEM and an example of BSE image of the fibre-matrix interface. (B) Clustering error as a function of the number of clusters. (C) All phases and (D) UH cement grains and pores segmented with the *k*-means clustering algorithm. Image segmentation follows the procedure reported in Ref. [10].

3 | RESULTS AND DISCUSSION

According to the Figure 2A and B, the ITZ can be identified by a reduction in porosity and an increase in UH grains with the distance from the fibre surface. The area fraction of pores demonstrated an increment with a decrease in fibre surface roughness (Figure 2A). In the case of polished fibres, the area fraction of porosity within 100 µm from fibre surface was greater than that of bulk cement paste, which was supported with Figure 3, revealing voids with an area larger than 0.02 mm^2. The porosity of the bulk cement paste was measures by applying same image analysis algorithm for 50 images of the cementitious matrix at a distance of minimum 200 µm from fibre surface. These voids were predominantly formed due to water agglomeration along the polished fibre surface. Results reported in Table 1 confirmed that lower values of fibre surface roughness increased the receding contact angle between water and fibre surface. This suggests poor sticking/adherence of water to the fibre surface, leading to nonuniform wetting of its surface.

However, the effect of the fibre surface roughness on the distribution of UH grains was not clearly indicated with the current measurements (Figure 2B). In the case of sanded fibres, the area fractions of both UH grains and porosity aligned with values measured in bulk

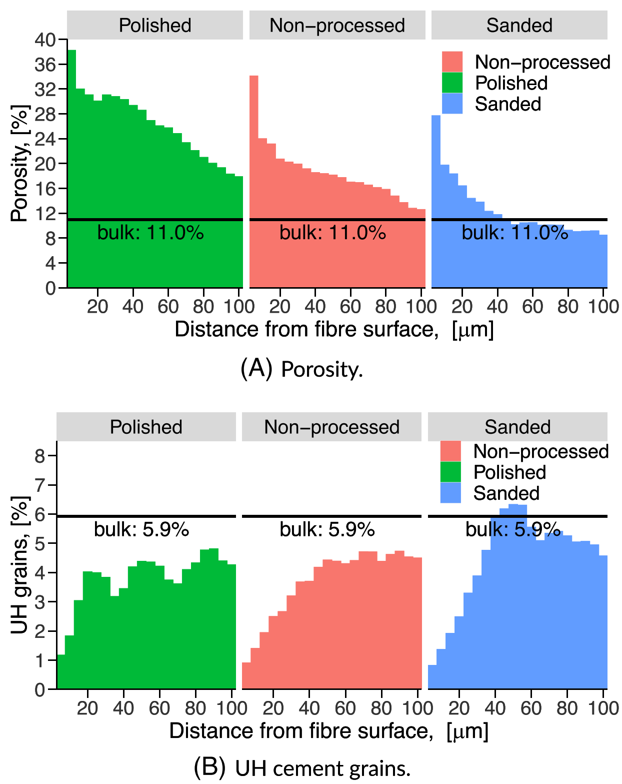

FIGURE 2 Average distributions of the pores and UH cement grains with the distance from the surface of the fibres with different roughness. Results are adopted from Ref. [10].

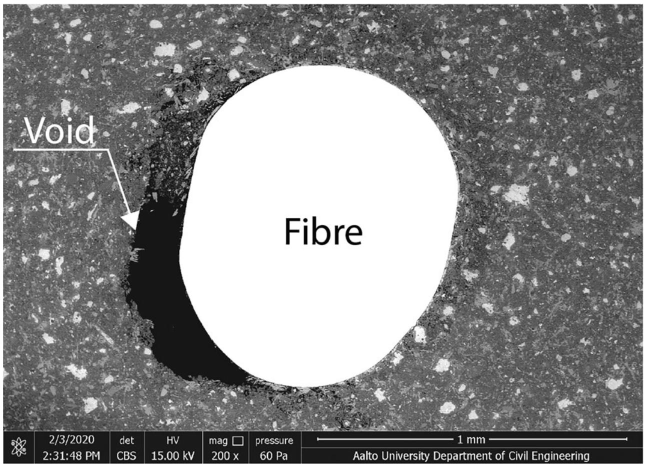

FIGURE 3 BSE images of the cross-section of the fibres with different types of surface roughness embedded in the cement paste.

TABLE 1 The results of fibre surface roughness (R_q), receding water contact angle on fibre surface (θ_r) and maximum pull-out strength on the fibre-matrix bond (F_{max}).

Fibre surface	R_q (μm)	θ_r	F^{max} (N)
Polished	0.031	52°	196
Nonprocessed	0.191	35°	291
Sanded	2.667	15°	450
References	10	10	11

R_q, root mean square roughness of fibre surface; θ_r, ability of water to stick on wet surface.

cement paste at a distance of 45 µm from the fibre surface.

The results of the cyclic pull-out test demonstrated in Table 1 also revealed a growth of strength of the fibre-matrix bond with an increase in fibre surface roughness. The analysis of the residual slip after each loading cycle in Figure 4 indicated the prolonged development of the residual slip increment until the accelerated evolution of damage (last 4 cycles) with an increase in fibre surface roughness. The increment in bond strength suggests the shift in pattern of the debonding crack, which can pass along the fibre surface or through the cement matrix. Based on Figure 5D–F, the amount of the cement paste adhered on the surface of the pulled out fibres increased with a growth of the surface roughness. This may be attributed to the changes in the ITZ microstructure formed near the fibres with different surface roughness. The higher roughness of the fibre surface redirects the debonding crack from the fibre-matrix interface further into the matrix (Figure 5G–I), where porosity is lower compared to the region at the fibre surface (Figure 2A). Therefore, increased roughness of the fibre surface contributes to the growth in the maximum capacity of the fibre-matrix bond.

4 | CONCLUSIONS

The provided summary of previous studies reported in Refs. [10, 11] confirmed, that the utilisation of SEM enabled to indicate the significance of fibre surface roughness on the changes in the distribution of surrounding porosity and UH grains. The increase in fibre surface roughness facilitated the uniform wetting of fibres, leading to a reduction in the porosity near fibre surface. As a result, the maximum capacity of the bond between the cement paste and fibres with different surface roughness, examined under direct tension cycles with gradually increasing amplitudes, increased with the growth of fibre surface roughness. The effect of the properties of fibre surface and cement paste surrounding it on the performance of the fibre-matrix bond were highlighted and introducing novel insights about the fibre-matrix interaction were introduced.

The understanding of the fibre-matrix bond reported can further be applied to the development of the FRCC by modifying the bond between the cementitious matrix and fibres or reinforcement bars of any material. In addition, the application of the k-means clustering algorithm for image segmentation demonstrated in this study can be

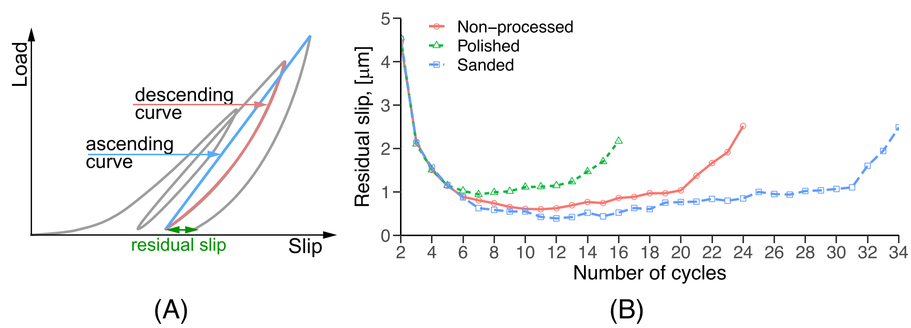

FIGURE 4 (A) Scheme of residual slip interpretation. (B) Residual slip development under cyclic loading of fibres with different surface roughness. Results and scheme are adopted from Ref. [11].

Journal of Microscopy RMS

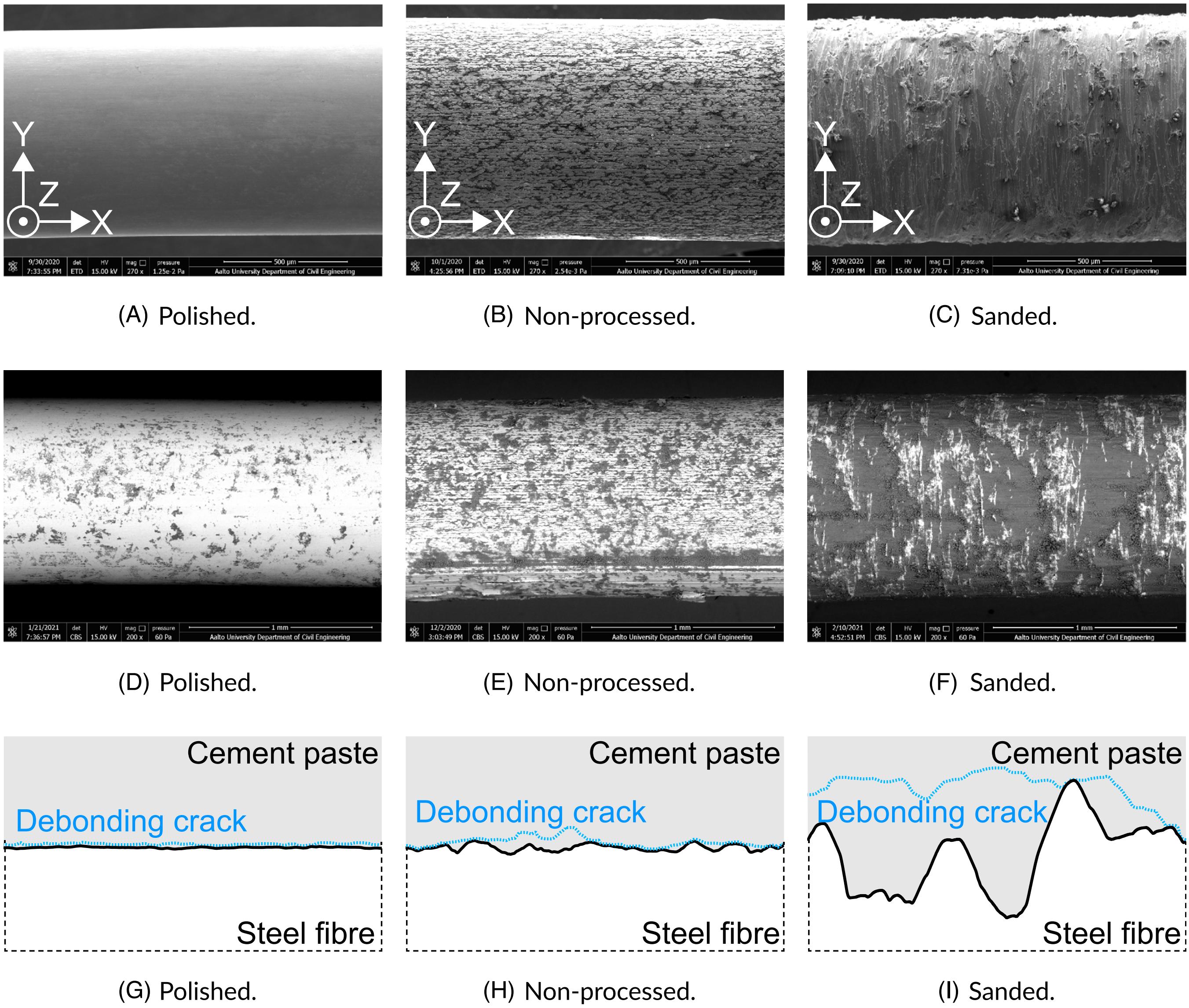

FIGURE 5 (A–C) SE images of the processed fibre surfaces before being embedded in cement paste (adopted from Ref. [10]). (D–F) Examples of the BSE images of the surfaces of the pulled out fibres. (G–I) The schematic pattern of the debonding crack along the fibres with different surface roughness.

used further for a wide range of research investigations, which rely on image analysis.

ACKNOWLEDGEMENTS

The research was funded by the AaltoENG doctoral programme of the School of Engineering of Aalto University.

ORCID

Anna Antonova https://orcid.org/0000-0002-2448-6477

REFERENCES

1. Lee, S. F., & Jacobsen, S. (2011). Study of interfacial microstructure, fracture energy, compressive energy and debonding load of steel fiber-reinforced mortar. *Materials and Structures*, *44*(8), 1451–1465.
2. Wang, X. H., Jacobsen, S., He, J. Y., Zhang, Z. L., Lee, S. F., & Lein, H. L. (2009). Application of nanoindentation testing to study of the interfacial transition zone in steel fiber reinforced mortar. *Cement and Concrete Research*, *39*(8), 701–715.
3. Pinchin, D., & Tabor, D. (1978). Interfacial phenomena in steel fibre reinforced cement II: Pull-out behaviour of steel wires. *Cement and Concrete Research*, *8*(2), 139–150.
4. Scrivener, K. L., Crumbie, A. K., & Laugesen, P. (2004). The interfacial transition zone (ITZ) between cement paste and aggregate in concrete. *Interface Science*, *12*(4), 411–421.
5. Gray, R., & Johnston, C. (1984). The effect of matrix composition on fibre/matrix interfacial bond shear strength in fibre-reinforced mortar. *Cement and Concrete Research*, *14*(2), 285–296.
6. Laranjeira, F., Aguado, A., & Molins, C. (2010). Predicting the pullout response of inclined straight steel fibers. *Materials and Structures*, *43*, 875–895.

7. Zhan, Y., & Meschke, G. (2014). Analytical model for the pull-out behavior of straight and hooked-end steel fibers. *Journal of Engineering Mechanics*, *140*(12), 04014091.
8. Li, B., Xu, L., Chi, Y., Huang, B., & Li, C. (2017). Experimental investigation on the stress-strain behavior of steel fiber reinforced concrete subjected to uniaxial cyclic compression. *Construction and Building Materials*, *140*, 109–118.
9. Sima, J. F., Roca, P., & Molins, C. (2008). Cyclic constitutive model for concrete. *Engineering Structures*, *30*(3), 695–706.
10. Antonova, A., Eik, M., Jokinen, V., & Puttonen, J. (2021). Effect of the roughness of steel fibre surface on its wettability and the cement paste close to fibre surface. *Construction and Building Materials*, *289*, 123139.
11. Antonova, A., Eik, M., & Puttonen, J. (2022). Importance of the surface roughness of a steel fibre pulled out from cement paste by slowly increasing load cycles. *Cement and Concrete Composites*, *134*, 104799.
12. Scrivener, K. L., Patel, H. H., Pratt, P. L., & Parrott, L. J. (1986). Analysis of phases in cement paste using backscattered electron images, methanol adsorption and thermogravimetric analysis. *MRS Proceedings*, *85*, 67.
13. Wong, H., Head, M., & Buenfeld, N. (2006). Pore segmentation of cement-based materials from backscattered electron images. *Cement and Concrete Research*, *36*(6), 1083–1090.
14. Gao, Y., Schutter, G. D., Ye, G., Huang, H., Tan, Z., & Wu, K. (2013). Porosity characterization of itz in cementitious composites: Concentric expansion and overflow criterion. *Construction and Building Materials* (Vol. *38*, pp. 1051–1057). 25th Anniversary Session for ACI 228 – Building on the Past for the Future of NDT of Concrete.
15. Likas, A., Vlassis, N., & J.Verbeek, J. (2003). The global k-means clustering algorithm. *Pattern Recognition*, *36*(2), 451–461. Biometrics.
16. Distante, A., & Distante, C. (2020). *Image segmentation* (pp. 271–332). Springer International Publishing, Cham.

How to cite this article: Antonova, A., Eik, M., & Puttonen, J. (2024). Characterisation of bond between cement paste and steel fibres with different surface roughness using SEM. *Journal of Microscopy*, *294*, 233–238. https://doi.org/10.1111/jmi.13298